ECOLOGY LETTERS

Ecology Letters, (2014) **17**: 670–679 doi: 10.1111/ele.12268

LETTER

The gliding speed of migrating birds: slow and safe or fast and risky?

Nir Horvitz,[1*†] Nir Sapir,[1†] Felix Liechti,[2] Roni Avissar,[3] Isaac Mahrer[4] and Ran Nathan[1]

Abstract

Aerodynamic theory postulates that gliding airspeed, a major flight performance component for soaring avian migrants, scales with bird size and wing morphology. We tested this prediction, and the role of gliding altitude and soaring conditions, using atmospheric simulations and radar tracks of 1346 birds from 12 species. Gliding airspeed did not scale with bird size and wing morphology, and unexpectedly converged to a narrow range. To explain this discrepancy, we propose that soaring-gliding birds adjust their gliding airspeed according to the risk of grounding or switching to costly flapping flight. Introducing the Risk Aversion Flight Index (RAFI, the ratio of actual to theoretical risk-averse gliding airspeed), we found that inter- and intraspecific variation in RAFI positively correlated with wing loading, and negatively correlated with convective thermal conditions and gliding altitude, respectively. We propose that risk-sensitive behaviour modulates the evolution (morphology) and ecology (response to environmental conditions) of bird soaring flight.

Keywords

Atmospheric modelling, bird migration, convective thermals, flight behaviour, movement ecology, risk-sensitive flight, soaring flight, tracking radar, turbulence kinetic energy, wing loading.

Ecology Letters (2014) **17**: 670–679

INTRODUCTION

Bird airspeed (horizontal speed relative to air) is arguably the most important component of flight performance shaping aerial movements of all kinds including long-distance migration (Pennycuick 2008). However, little is known about how evolutionary and ecological factors modulate the airspeed of free-ranging migrating birds. More than 300 bird species of various taxonomic groups undertake long migratory journeys using soaring-gliding flight mode (Del Hoyo *et al*. 1992). This mode of flight is composed of alternating phases of soaring, in which the bird ascends by circling within rising air columns, usually created by the heating of the surface (hereafter, 'thermals'), and gliding, in which the bird progresses towards its destination while losing height until it encounters another thermal and ascends within it. Thermals may be recognised by clouds often created above them, and by observing other circling birds nearby (Pennycuick 1978). According to aerodynamic theory, both the gliding airspeed (V_a) and the sink rate (V_z, the rate of altitude loss) of a gliding bird are determined by the bird's gliding angle, a relationship known as the glide polar (Reichmann 1978; Pennycuick 2008; Fig. 1a). Birds may fly at specific gliding airspeed within the range determined by their glide polar by controlling their angle of descent through adjustments of their body posture and wing flexion (Tucker 1987).

Two points on the glide polar represent alternative behavioural strategies along the V_a spectrum (MacCready 1958; Pennycuick 1972) with implications for flight performance (Figs 1a and S1). The first, the best glide speed (V_{bg}), represents the highest ratio of V_a to V_z, maximising the gliding distance. The second, the optimal ('speed-to-fly') speed (V_{opt}), is derived from the MacCready theory (MacCready 1958). According to this theory, gliding at V_{opt} maximises bird cross-country speed (overall flight speed with respect to the desired destination) by adjusting the gliding airspeed to the rate of ascent at the preceding soaring phase. Thus, V_{bg} is independent of the rate of ascent, whereas V_{opt} increases with ascent rate. The MacCready theory suggests that, everything else being equal, a bird (or a glider) aiming to maximise its cross-country speed should glide at V_{opt}.

Yet, the MacCready theory does not take into account the stochastic nature of thermals, assuming that thermals are always available and that bird climb rate will be similar for two consecutive thermals. Since gliding at V_{opt} involves a greater rate of descent and thus higher probability of reaching the ground before encountering a thermal for ascent (Pennycuick 2008; Fig. 2), gliding at V_{opt} entails a greater risk of forced landing or switching to a more energy-consuming flapping flight (hereafter, 'grounding/flapping risk'). Due to the stochastic distribution of convective thermals in time and space (Pennycuick 1978; Bradbury 2000), gliding birds should consider the grounding/flapping risk of not encountering a thermal during the gliding phase (Fig. 2). A risk-averse bird is expected to glide at V_{bg} to increase its gliding duration, at the

[1]*Movement Ecology Laboratory, Department of Ecology, Evolution and Behavior, Alexander Silberman Institute of Life Sciences, Edmond J. Safra campus, The Hebrew University of Jerusalem, 91904, Jerusalem, Israel*
[2]*Swiss Ornithological Institute, CH-6204, Sempach, Switzerland*
[3]*Rosenstiel School of Marine and Atmospheric Science, University of Miami, 4600 Rickenbacker Causeway, Miami, FL, 33149, USA*
[4]*The Seagram Center for Soil and Water Sciences, The Robert H. Smith Faculty of Agriculture, Food and Environment, The Hebrew University of Jerusalem, P.O. Box 12, 76100, Rehovot, Israel*
**Correspondence: E-mail: nir.horvitz@mail.huji.ac.il*
†These authors contributed equally to this work.

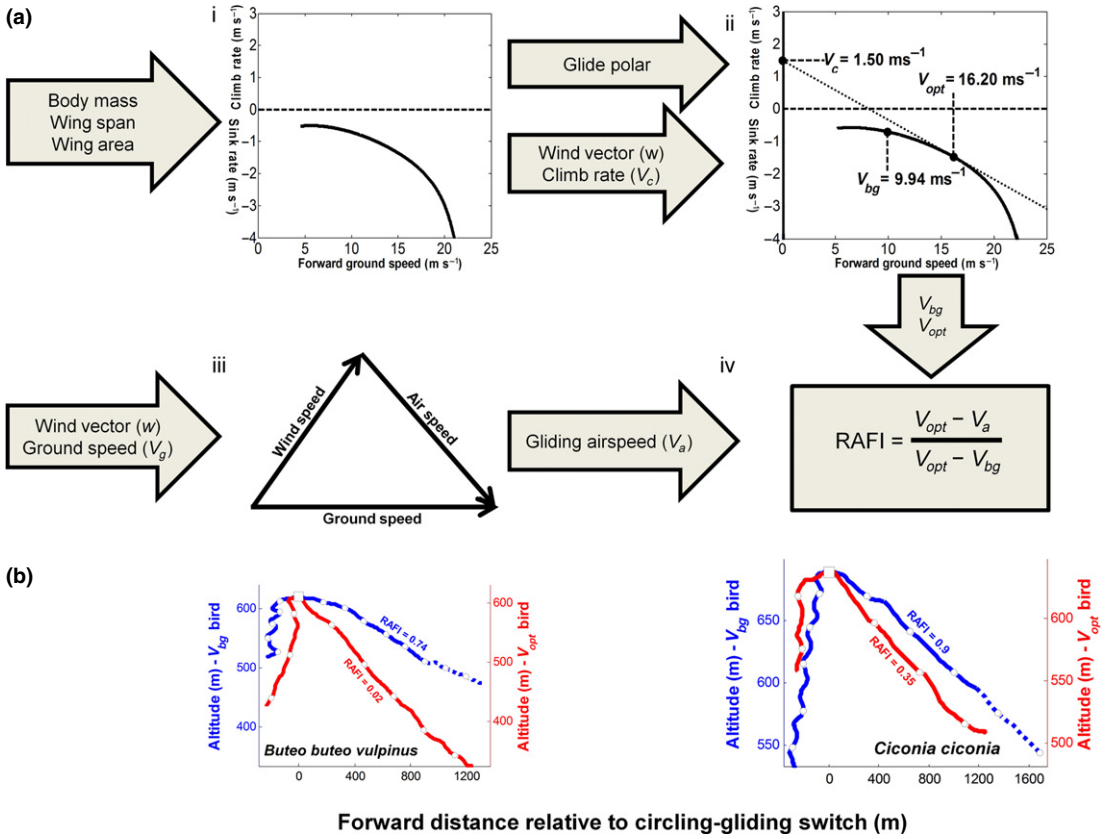

Figure 1 Risk Aversion Flight Index (RAFI) computation and examples. (a) RAFI calculation flow chart: glide polar calculations using biometric traits (i), wind vector (w) and climb rate (V_c) (ii) to compute V_{bg} and V_{opt}. Gliding airspeed (V_a) is retrieved by subtracting the wind vector (w) from the bird's vector (iii) to calculate RAFI based on V_a position along the V_{bg} to V_{opt} spectrum (iv). (b) Examples of recorded flight tracks. Blue lines and left ordinates represent birds gliding closer to V_{bg}, (high RAFI); red lines and right ordinates represent birds gliding closer to V_{opt} (lower RAFI). Open squares (zero value on the abscissa) represent the switching point between circling and gliding, and open circles represent bird location at 20 s intervals before and after this point. Solid lines represent equal duration of gliding for the two birds, and dashed blue line is the remaining recorded gliding of the V_{bg} bird.

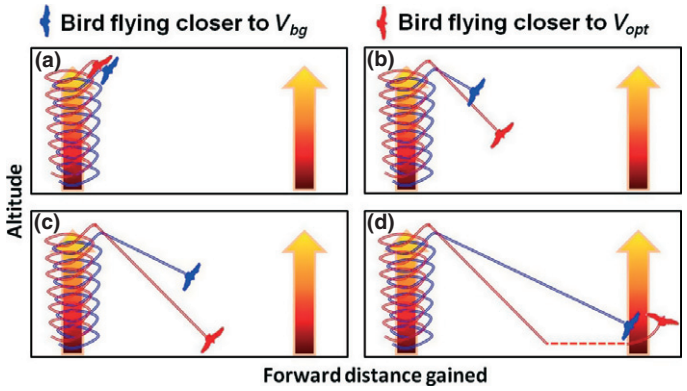

Figure 2 Illustration of risk-sensitive gliding flight of migrating birds. (a) Two birds soar to the top of a convective thermal and start gliding from the same height at either V_{opt} (red) or V_{bg} (blue). (b) The V_{opt} bird glides faster, gaining more distance but losing more height. (c) The V_{opt} bird reaches the ground before finding a thermal suitable for ascent and must therefore either land or switch to energetically costly flapping flight. (d) The V_{bg} bird finds a thermal suitable for ascent and starts circling to gain height.

cost of a slower progress, whereas a risk-prone bird would glide at V_{opt} to progress more rapidly to its destination, at a higher grounding/flapping risk. Grounding/flapping risk is especially important for heavier birds for which the cost of flapping is considerably higher (Pennycuick 2008). Also, the grounding/flapping risk is probably crucial during enduring long-distance migration due to the poor body condition of many migrants, giving rise to strong selection pressures to minimise the cost of transport (Alerstam & Lindström 1990; Alerstam 1991; Hedenström 1993). Previous studies have placed the recorded V_a of migrating birds in reference to the two endpoint values, V_{bg} and V_{opt} (Pennycuick 1972, 1978; Bruderer *et al.* 1995; Liechti *et al.* 1996; Spaar & Bruderer 1997), or to V_{opt} alone (e.g. Ákos *et al.* 2008). Yet, these studies have not accounted for the factors explaining the variance in V_a among species and individuals, overlooking evolutionary and ecological factors that may shape the gliding airspeed of migrating birds.

To discern the factors affecting the gliding flight performance of migratory birds, we combined high-resolution (1 s sampling interval, 1–10 m accuracy depending on distance) radar tracking (Bruderer *et al.* 1995; Liechti *et al.* 1996; Spaar & Bruderer 1997; Fig. 1b), glide polar calculations for each bird based on species size and morphology, and numerical atmospheric simulations by the Regional Atmospheric Modeling System (RAMS, Pielke *et al.* 1992; Walko *et al.* 2000; Cotton *et al.* 2003). We used RAMS to estimate the wind

vectors that each individual bird encountered during flight, focusing on distinct events of soaring followed by gliding (Figs 1 and 2). Our sample is composed of 1346 migrating birds of 12 different species that vary substantially in their body mass and wing morphology (Bruderer & Boldt 2001; Bruderer *et al*. 2010; Table 1).

To assess risk-sensitive gliding flight with respect to the grounding/flapping risk, we introduce the Risk Aversion Flight Index (RAFI; Fig. 1a), which represents the relative position of the bird's actual gliding airspeed on the theorised V_{bg} to V_{opt} spectrum (i.e. RAFI = $(V_{opt} - V_a)/(V_{opt} - V_{bg})$, see Materials and Methods). The highest theorised index value (RAFI = 1) represents a risk-averse bird gliding at V_{bg}, a relatively slow flight lowering the grounding/flapping risk. The lowest theoretical value (RAFI = 0) represents a risk-prone bird gliding at V_{opt}, a fast flight associated with high grounding/flapping risk (Figs 1a and 2).

In the following, we contrasted two sets of alternative predictions, the first derived from bird aerodynamic theory and current knowledge, the second from our risk-sensitive flight hypothesis. For instance, prediction 1a, derived from aerodynamics theory was contrasted with its alternative prediction 1b, derived from our hypothesis. We thus predict that: (1a) mean species' V_a will increase with wing loading because both V_{bg} and V_{opt} increase with wing loading (Hedenström & Alerstam 1998; Pennycuick 2008); alternatively, (1b) RAFI will be lower (i.e. V_a closer to V_{opt}) for birds with lower wing loading and high (i.e. V_a closer to V_{bg}) for birds with high wing loading, resulting in no increase in species' V_a with wing loading; (2a) mean species' V_a will fit either V_{bg} or V_{opt} following past studies (Pennycuick 1972, 1978; Bruderer *et al*. 1995; Liechti *et al*. 1996; Spaar & Bruderer 1997; Ákos *et al*. 2008); alternatively, (2b) due to the risk-sensitive response predicted in 1b, mean species' V_a will not necessarily fit either V_{bg} or V_{opt} but will vary in a predictable manner between V_{bg} (minimum) to V_{opt} (maximum); (3a) V_a will be higher when thermal intensity, or the height of the bird at the end of the soaring phase (which may be the outcome of thermal intensity), are higher and will follow V_{opt} according to the MacCready theory. Accordingly, RAFI will be zero, or near zero (bird gliding airspeed will be equal to V_{opt}), regardless of thermal intensity or the height of the bird at the end of the soaring phase; alternatively, (3b) RAFI will decrease (bird gliding airspeed will become closer to V_{opt}) with thermal intensity and the height of the bird at the end of the soaring phase. In addition, following recent evidence (Nilsson *et al*. 2013) that, unlike other bird groups, thermal soaring birds do not migrate faster in spring than they do in autumn, we also predict that (4) RAFI will not differ between the seasons. Finally, as winds can strongly influence bird flight behaviour (Liechti 2006), we also tested the effects of tailwind assistance and cross-winds on RAFI. Such effects are likely to be complex; for instance, wind assistance may enable faster glide between thermals, but concomitantly may break down thermals due to air mixing and thus may reduce thermal availability (Kerlinger 1989; Duerr *et al*. 2012). Therefore, we do not provide *a priori* predictions for wind effects on RAFI.

MATERIALS AND METHODS

Study sites

Flight tracks of migrating birds were collected at two sites: Sede Boqer (N 30°51′26″ E 34°48′02″) and Idan (N 30°49′10″ E 35°16′00″), both of which are located in the Negev Desert of southern Israel, ~ 45 km apart, within a main soaring bird migration flyway (Bruderer *et al*. 1995; Spaar & Bruderer 1996, 1997). The two study sites differ from one another topographically. The Idan site (−160 m ASL) is located on an open and relatively wide plateau within the Arava Valley, whereas the Sede Boqer site is located in a region of complex terrain neighbouring the wide gorge of Wadi Zin within the Negev highlands (470 m ASL).

Tracking radar

'Superfledermaus' radars, which are capable of tracking small migrating birds from a distance of 5 km and up to 8 km for larger birds, were used for bird tracking (Bruderer *et al*. 1995). The maximal distance error of these radars is ± 10 m and the maximal azimuth and elevation error is ± 0.06º (Bruderer & Boldt 2001). Each radar was connected to a computer using custom-made software that registered the three-dimensional position of the tracked bird every second. To identify the species of bird, an experienced observer identified the tracked target through a 12.4× magnifying telescope that was mounted parallel to the radar antenna. Birds were tracked during a total of 171 tracking days in the two sites during the spring and fall of 1991 and 1992.

Atmospheric simulations

Atmospheric data were simulated by the RAMS (Pielke *et al*. 1992; Walko *et al*. 2000; Cotton *et al*. 2003), which has been widely employed for atmospheric studies at various temporal and spatial scales, from seconds and several metres to decades and an entire continent. Our RAMS application contained four nested grids, with a finest grid cell size of 250 m × 250 m (Fig. S2). The temporal resolution of the simulation output was one minute. For model input, we used the European Centre for Medium-Range Weather Forecasts (ECMWF) mandatory-level reanalysis, produced every 6 h at a 2.5° spatial resolution worldwide, and a 250 m resolution digital elevation model produced by the Hebrew University GIS centre. See Sapir *et al*. (2011) for validation data of our RAMS simulations. We made use of three parameters of the RAMS output in our analyses. The first two, wind U (west-east) and V (south-north) components were used to calculate gliding airspeed (Fig. 1). The third, turbulence kinetic energy (TKE), was used as a proxy of thermal intensity. TKE in the mid-section of the planetary boundary layer is a commonly used proxy for convective updraft intensity (Mandel *et al*. 2008; Sapir *et al*. 2011) because convective air movement is characterised by highly turbulent flow (Stull 1988).

Table 1 Species-specific morphological attributes, theoretical V_{bg} and V_{opt}, observed V_a, Risk Aversion Flight Index (RAFI; *cf.* Table S1), climb rate and circling radius.

Species	Abbreviation	Body mass (kg)	Wingspan (m)	Wing area (m^2)	Wing loading (kg m^{-2})	Aspect ratio	# of paired tracks	Mean ± STD V_a (ms^{-1})	Theoretical V_{bg} (ms^{-1})	Mean ± STD theoretical V_{opt} (ms^{-1})	Mean RAFI	Mean ± STD climb rate (ms^{-1})	Mean ± STD circling radius (m)
Black stork *Ciconia nigra*	BS	3.000	1.850	0.500	6.000	6.845	15	12.85 ± 3.83	12.66	19.14 ± 2.73	0.999	1.43 ± 0.58	13.01 ± 2.20
White stork *Ciconia ciconia*	WS	3.600	2.160	0.651	5.530	7.169	49	14.19 ± 4.16	13.67	20.64 ± 2.92	0.946	1.61 ± 0.73	11.68 ± 2.62
Honey buzzard *Pernis apivorus*	HB	0.800	1.270	0.260	3.077	6.203	211	13.83 ± 3.68	9.83	15.60 ± 1.91	0.29	1.57 ± 0.64	10.72 ± 2.49
Black kite *Milvus migrans*	BK	0.858	1.400	0.274	3.131	7.143	80	13.59 ± 3.43	9.98	16.05 ± 2.21	0.429	1.54 ± 0.72	10.18 ± 2.81
Marsh harrier *Circus aeruginosus*	MaH	0.651	1.330	0.225	2.893	7.869	52	13.24 ± 2.89	9.54	16.22 ± 1.42	0.45	1.57 ± 0.60	10.05 ± 1.49
Montagu's harrier *Circus pygargus*	MoH	0.300	1.125	0.146	2.055	8.651	15	12.59 ± 2.10	6.93	12.76 ± 1.74	0.004	1.30 ± 0.57	11.03 ± 1.24
Levant sparrowhawk *Accipiter brevipes*	LS	0.220	0.700	0.074	2.973	6.631	94	14.09 ± 3.80	10.04	15.76 ± 2.19	0.258	1.66 ± 0.71	10.24 ± 2.21
Steppe buzzard *Buteo buteo vulpinus*	SB	0.580	1.190	0.207	2.802	6.841	502	14.70 ± 3.49	9.44	15.41 ± 1.97	0.109	1.61 ± 0.68	10.62 ± 2.80
Lesser spotted eagle *Aquila pomarina*	LSE	2.015	1.800	0.513	3.928	6.312	111	15.39 ± 3.61	11.49	17.67 ± 2.69	0.397	1.63 ± 0.73	11.37 ± 2.41
Steppe eagle *Aquila nipalensis*	SE	2.900	2.025	0.485	5.979	8.450	159	14.16 ± 3.88	12.34	20.32 ± 3.09	0.82	1.65 ± 0.76	12.52 ± 2.33
Booted eagle *Hieraaetus pennatus*	BE	0.595	1.160	0.200	2.975	6.715	46	12.86 ± 4.29	9.2	14.77 ± 2.17	0.406	1.41 ± 0.62	10.77 ± 2.70
European bee-eater *Merops apiaster*	EBE	0.058	0.470	0.027	2.148	8.092	12	14.03 ± 3.58	8.57	14.1o3 ± 1.46	0.049	1.52 ± 0.47	9.30 ± 2.87

Formally, wing loading is force (i.e. weight, not mass) per unit area in units of N m^{-2} and we retained the common definition of mass per unit area in kg m^{-2} (Alerstam *et al.* 2007; Pennycuick 2008). Multiplying our values by 9.81 (m s^{-2}, acceleration due to gravity) will provide the formal wing loading values in N m^{-2}. The morphological attributes of the 12 species were used for calculating the glide polar of each species. A paired track is a thermal circling phase followed by a gliding phase (see Materials and Methods). The theoretical V_{opt} statistics were calculated from the species' specific glide polar formula and the calculated climbing rate while circling before the start of gliding.

Identifying thermal circling during soaring and gliding

We defined a part of a track as a soaring phase if it included continuous change in heading angle in one direction during at least two full circles, if at least 80% of the bird's vertical 1 s steps were upward and at least 80% of the horizontal 1 s steps showed a circling pattern for at least 20 s. Similarly, a gliding phase was recognised if 80% of the 1 s steps were downwards without circling for at least 20 s. Because RAFI calculations necessitate computing the theoretical V_{opt} during gliding based on the climb rate at the preceding thermal soaring phase, we only used tracks consisting of soaring immediately followed by gliding. We calculated bird circling radius during soaring using three consecutive coordinates during a single circle and averaged all radii calculated during a single soaring phase.

Calculating bird air and ground speed

The ground speed of a bird during time interval $t_2 - t_1$ was calculated as the horizontal displacement divided by time

$$V_g = \frac{\sqrt{(x_2 - x_1)^2 + (y_2 - y_1)^2}}{t_2 - t_1}, \quad (1)$$

where x_t and y_t are the x and y coordinates of the bird at time t, respectively, and assuming that $t_2 - t_1$ is small enough (1 s in this study). The gliding airspeed (V'_a) was calculated by subtracting the wind vector from the ground speed vector (Fig. 1A)

$$V'_a = V_g - w, \quad (2)$$

where w, the wind vector, is considered constant between t_1 and t_2 (i.e. winds experienced by the bird do not vary between t_1 and t_2). Because the 1346 bird tracks we analysed encompass different flight altitudes, we used the equivalent gliding airspeed of the bird to make them comparable (Pennycuick 2008). Equivalent gliding airspeed is calculated by dividing the gliding airspeed by the square root of the ratio of air density at bird position to the air density at sea level:

$$V_a = V'_a \sqrt{\frac{\rho}{\rho_0}}, \quad (3)$$

where ρ is the air density at the altitude of the bird and ρ_0 is the air density at sea level. We use only the equivalent gliding airspeed V_a throughout the paper.

Calculating bird glide polar, V_{bg}, V_{opt} and RAFI

We calculated the birds' theoretical V_{bg} and V_{opt} using equations given in Pennycuick (2008) and species' morphology (Table 1). We compared our results with those obtained for the same input values from the Flight (version 1.23) software (http:/www.bristol.ac.uk/biology/media/pennycuick.c/flight_123.zip) and found no differences. RAFI is computed as the relative position of the bird's actual gliding airspeed (V_a) on the interval between its theorised V_{bg} and V_{opt} (Fig. 1a):

$$RAFI = \frac{V_{opt} - V_a}{V_{opt} - V_{bg}}. \quad (4)$$

Species-specific RAFI values are the means of all the RAFI values calculated from the tracks of all individuals of a certain species. We note that birds can glide faster than V_{opt} or slower than V_{bg} but such rare cases involving extreme slow or fast airspeeds likely cancel each other and have little, if any, effect on mean species' V_a.

Data analysis

We applied regressions using linear ($y = ax + b$) and logarithmic ($y = a \log x + b$) models to test the relationships between morphological traits (body mass, wing area, wingspan, aspect ratio that is the square of the wingspan divided by the wing area and wing loading that is the body mass divided by the wing area), and RAFI, V_a and circling radius. The regressions were computed using the phylogenetically controlled generalised least squares method (Garland & Ives 2000) to minimise the effects of phylogenetic bias. Phylogenetic data were taken from Griffiths *et al.* (2007) and Hackett *et al.* (2008). The best model was selected based on the lowest Akaike information criterion value, modified for small sample sizes (Burnham & Anderson 2002). Pearson correlation was used to test the correlation between the five morphological traits. To study how intraspecific variation in morphological traits may affect these relationships, we calculated mean V_a by bootstrapping RAFI through incorporation of realistic estimates of intraspecific variation in bird biometric attributes. Testing the relationships between RAFI and both TKE and the height where birds started to glide (hereafter gliding height) was done by an analysis of covariance (ANCOVA) that included both categorical (species) and continuous (TKE or gliding height) explanatory variables. An ANCOVA was also applied to examine the effects of bird species and TKE on bird climb rate during soaring, and the effects of tailwind assistance and cross-winds on RAFI. We used a two-way ANOVA to test the effects of bird species and season (spring or fall) on RAFI. All statistical analyses were done in Matlab version 7.14 (MathWorks Inc, Natick, MA, USA).

RESULTS

We found no support for some of the most basic scaling relationships of soaring-gliding flight derived from aerodynamic theory, predicting that gliding airspeed increases with body mass, wing loading or any other wing morphology parameters. Mean V_a was not significantly related to wing loading ($P = 0.71$), body mass ($P = 0.56$) or any other morphological attribute ($P > 0.26$ for all parameters). Moreover, the expected range of mean V_a of the different species based on the species-specific glide polars when examining V_{bg} alone (6.8 ms^{-1}, 6.9–13.7 ms^{-1}), V_{opt} alone (7.9 ms^{-1}, 12.7–20.6 ms^{-1}) or the entire range of both V_{bg} and V_{opt} (13.7 ms^{-1}, 6.9–20.6 ms^{-1}) is substantially (2.7–5 times) wider than the observed mean V_a range (2.7 ms^{-1}, 12.5–15.2 ms^{-1}). Although our biometric data are averaged per species and not

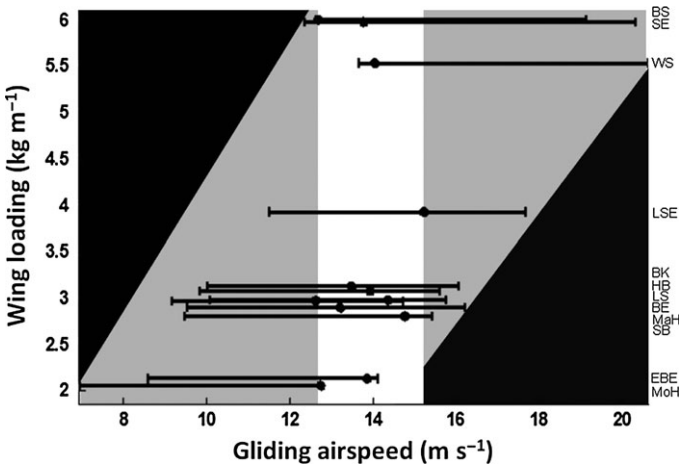

Figure 3 Convergence of gliding airspeed. Actual gliding airspeed (V_a) converged to a narrow range of 2.7 ms^{-1} (white range in the middle) within the much larger theorised range of V_{bg} (best glide speed) and V_{opt} (optimal 'speed-to-fly' speed) spanning 13.7 ms^{-1}. For each species, the mean V_a is depicted by a black dot within a bar that indicates the species-specific range between V_{bg} and V_{opt} (left and right bar tips, respectively). Species abbreviations are given at the right of the figure (see Table 1).

specific for each recorded individual, bootstrapping the data with conservative estimates of intraspecific variance in body mass and wing morphometrics revealed robustness of our results to variability among individuals (Table S1; Fig. S3). Therefore, despite their markedly different morphology and size (Table 1), soaring-gliding bird species glide at similar gliding airspeeds because high wing loading species tend to fly close to their (relatively slow) V_{bg}, whereas low wing loading species fly close to their (relatively fast) V_{opt}, resulting in narrow V_a range (Fig. 3). These findings are in contrast to Predictions 1a and 2a.

We found that interspecific variation in RAFI was best explained by wing loading under a logarithmic model ($R^2 = 0.96$, $P < 0.001$; Fig. 4A; Tables S2 and S3). This implies that bird species with relatively high wing loading glide in a risk-averse manner, and those with relatively low wing loading would be risk prone. This finding supports Prediction 1b. The relationships between the other four morphological variables and RAFI are given in Figure S4, and the correlations between the five morphological traits are provided in Table S5. As previously suggested (Pennycuick 1972; Ákos *et al.* 2010), we also found that birds with lower wing loading can circle in a smaller radius during the soaring phase ($R^2 = 0.77$, $P < 0.001$; Fig. 4b; Table S4).

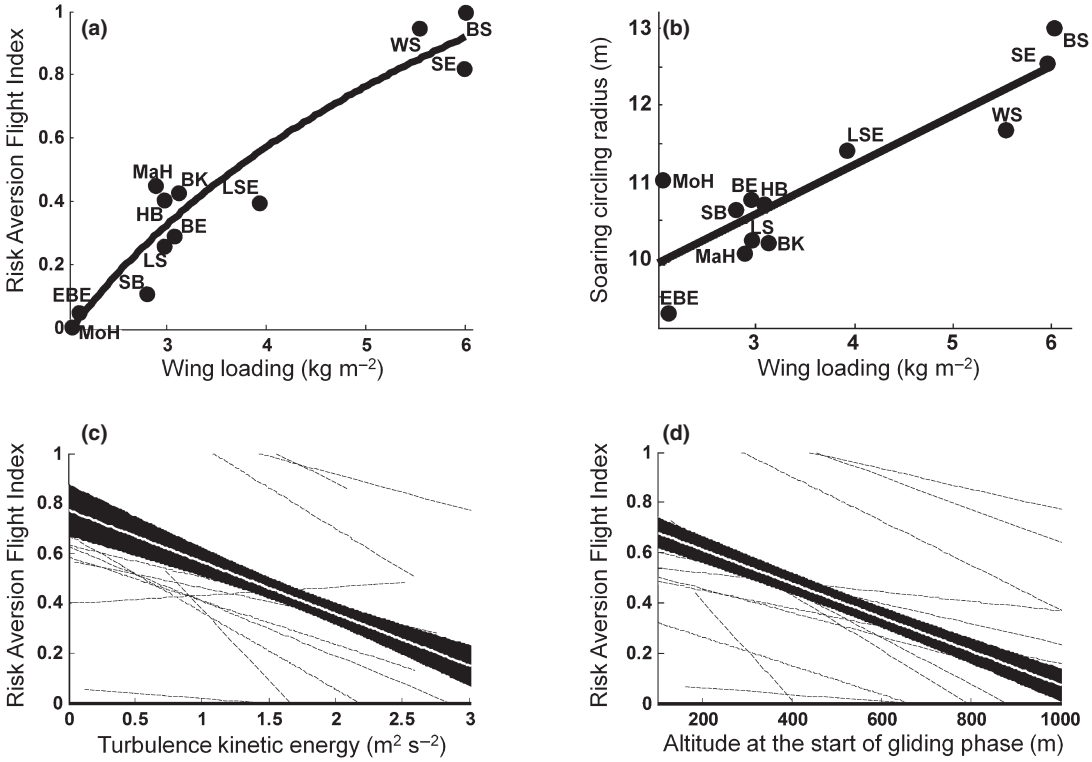

Figure 4 Body mass, wing morphology and atmospheric conditions strongly affect the Risk Aversion Flight Index (RAFI). (a) Interspecific variation in RAFI is explained by a logarithmic relationship with wing loading ($R^2 = 0.96$, $P < 0.001$; Tables S2 and S3). (b) Interspecific variation in circling radius while soaring is explained by a linear relationship with wing loading ($R^2 = 0.77$, $P < 0.001$; Table S4). Intraspecific variation in RAFI is explained by (c) thermal soaring conditions (turbulence kinetic energy, TKE, in the mid-section of the planetary boundary layer) and (d) the altitude in which gliding started. RAFI decreases with increasing TKE and flight altitude at the start of the gliding phase ($P < 0.001$ in both cases; Tables S5 and S6). The black area indicates 95% confidence bounds around the mean response calculated for all individuals of all species combined. Grey dashed lines are the species-specific regression lines.

To explore the ecological part of our risk-sensitive flight hypothesis, we tested the intraspecific relationships between RAFI and atmospheric conditions. Prior to these tests, we examined the common assumption that bird ascent rate during soaring is directly affected by thermal intensity (Pennycuick 2008). We found that, irrespective of species, bird climb rate is positively and highly significantly related to TKE ($P < 0.001$; Table S6). RAFI values were negatively related to both TKE and gliding height ($P < 0.001$ in both cases; Fig. 4c and 4d; Tables S7 and S8), and the same was found for V_a ($P = 0.003$ and $P < 0.001$ for TKE and gliding height respectively). These findings contrast Prediction 3a and support Prediction 3b. We found no significant seasonal effects on both RAFI ($P = 0.27$; Table S9) and V_a ($P = 0.17$; Table S9), supporting Prediction 4. In addition, no effects of tailwind assistance ($P = 0.57$) and cross-wind speed ($P = 0.44$) on RAFI were found.

The joint effects of bird morphology (wing loading) and the environment (TKE) on RAFI can be described by a simple equation ($\text{RAFI} = 4.5 + [-5.09 + 0.86\mathbf{log}(\text{wing loading})] \times \text{TKE}^{0.06}$), as illustrated in Figure 5. This figure offers an integrated, quantitative framework for the risk-sensitive flight hypothesis, predicting flight behaviour for different morphologies and environmental conditions. It also predicts the conditions for which flight might be too slow to allow progress at desirable speed, especially for high wing loading birds.

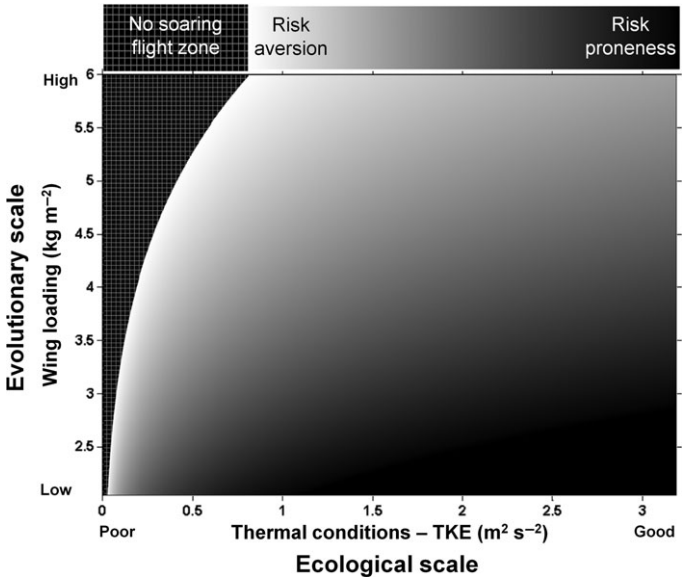

Figure 5 Ecological and evolutionary factors affecting the Risk Aversion Flight Index (RAFI). Wing loading, varying at an evolutionary timescale, and turbulence kinetic energy (TKE), varying at ecological/behavioural timescales, effects on RAFI. The resulting regression equation is $\text{RAFI} = 4.5 + [-5.09 + 0.86\log(\text{wing loading})] \times \text{TKE}^{0.06}$, fitted using all 1346 tracks. Regressed RAFI values are presented across the entire range, from white (RAFI = 1; extremely risk averse) to black (RAFI = 0; extremely risk prone). The TKE axis spans from 0 to the maximal simulated value (3.4 $m^2 s^{-2}$). Wing loading spans from the minimal (Montagu's harrier, 2.055 kg m^{-2}) to the maximal (Black stork, 6.000 kg m^{-2}) values among the study species. The black lattice depict RAFI values > 1, indicating conditions for which gliding airspeeds might be too slow to attain desirable progress speed and consequently may be avoided by soaring birds during migration, by either landing or flying at V_{bg} despite the higher grounding/flapping risk involved.

DISCUSSION

Aerodynamic theory, which applies principles of fluid mechanics to study the dynamics of the moving air and airborne objects mostly for guiding human aviation research, has been successfully applied also to study the flight of birds (Pennycuick 1969, 1972, 2008) and other flying organisms (Vogel 1966; Ellington 1984; Hedenström *et al.* 2007). Focusing on soaring-gliding migrating birds, we tested here some of the most basic theoretical predictions relating gliding airspeed to bird body mass and morphology, as well as to the theorised gliding airspeeds derived from the glide polar, including the optimal gliding speed predicted by the MacCready theory (MacCready 1958). Our tests revealed no support for some of the most basic theoretical expectations, whereas predictions derived from the risk-sensitive flight hypothesis introduced in this study were strongly supported.

The gliding airspeed of birds can be portrayed by the glide polar, predicting faster gliding for heavier birds and thus, due to the strong correlation with body mass, also for birds with higher wing loading. Although these theoretical relationships have long been recognised, empirical examinations based on comprehensive intra- and interspecific comparisons were lacking, presumably due to the practical challenge of accurately quantifying gliding airspeed (and not merely ground speed) across complete soaring-gliding cycles for a large number of individuals and species under variable real-life environmental conditions. Our analysis of high-resolution tracks of full soaring-gliding cycles consisting of 1346 migrating birds of 12 different species, combined with detailed atmospheric simulations to quantify gliding airspeed, revealed that, in contrast to theory, gliding airspeed neither scales with body mass nor with wing loading or other morphological parameters examined. Rather, gliding airspeeds of 12 species converged to a small range of 2.7 m s^{-1}, between 12.5 and 15.2 m s^{-1}, considerably narrower than theoretical expectations (Fig. 3).

To explain this unexpected result, recall that the glide polar does not predict one optimal gliding airspeed, but a range of potentially optimal ones that might correspond to different optimisation criteria. Although the two end points of this range, V_{bg} (the best glide speed that represents the highest ratio of gliding airspeed to sink rate, maximising the gliding distance) and V_{opt} (the optimal 'speed-to-fly' speed that maximises overall flight speed with respect to the desired destination by adjusting the gliding airspeed to the rate of ascent at the preceding soaring phase), are expected to increase with body mass (or wing loading), and the mean gliding airspeeds of all study species were included within their theoretical species-specific range, birds may choose to glide at various airspeeds within this range, not necessarily at one of the two endpoints or at some average value (*cf.* Pennycuick 1972, 1978; Bruderer *et al.* 1995; Liechti *et al.* 1996; Spaar & Bruderer 1997; Ákos *et al.* 2008). Because V_{opt} depends on the rate of climb during the preceding soaring phase (MacCready 1958), gliding airspeeds convergence could have been explained, at least partially, by the opposing effects of body

mass (or wing loading) on climb rate vs. gliding airspeed: lighter birds climb faster but glide slower. Yet, we found no support for this potential explanation, as the mean climb rate was also not significantly correlated with body mass, wing loading or any other morphological parameter ($P > 0.26$ for all parameters; see data in Table 1). Furthermore, the observed airspeed convergence range shifted to considerably lower values (by 17% on average), and was also three times narrower, compared to the expected V_{opt} range based on the MacCready theory (Fig. 3). Assuming that migrating birds attempt to maximise cross-country speed to minimise migration time (Alerstam & Lindström 1990; Alerstam 1991; Hedenström 1993) and hence are expected to glide at V_{opt}, why they do not fly as fast as they can?

This intriguing question, as well as the convergence of gliding airspeeds more generally, can all be explained by the risk-sensitive flight hypothesis introduced in this study. Although the idea that birds may glide in a risk-sensitive manner is not new (Pennycuick 1978; p. 175–176; Pennycuick 2008, p. 291–292), this concept has been greatly neglected in bird flight research, neither formalised nor quantitatively implemented in bird aerodynamic theory, and also not yet empirically tested. To formalise and test the risk-sensitive flight hypothesis, we introduced a simple index, denoted as RAFI, quantifying the level of risk aversion in bird gliding flight. Our hypothesis, formally defined in the Introduction, postulates that soaring-gliding birds choose their gliding airspeed considering the grounding/flapping risk associated with a failure to detect adequate thermals farther ahead. Among the two components of this risk, grounding is a common cost for both birds and glider pilots, whereas the cost of flapping is equivalent to activating the engine in motor gliders, entailing much higher energy expenditure compared to gliding. Both risk components depend on the joint effects of structural features (mass, morphology and design) and environmental conditions, which represent complementary evolutionary and ecological processes shaping flight performance in soaring-gliding birds, considered next.

Among the different bird structural features examined in this study, wing loading – the ratio of body mass to wing area – best explained variation in RAFI between species. This finding corresponds to the well-established significance of wing loading in soaring flight (Reichmann 1978; Hedenström & Alerstam 1998; Pennycuick 2008). We found that birds from species with lower wing loading soared in smaller circles (Pennycuick 1972; Ákos *et al*. 2010), suggesting an ability to utilise the strong lift at the centre of weak thermals, compared to birds from species with high wing loading that are limited to stronger and/or wider thermals (Fig. 4b). Furthermore, the cost of switching to flapping flight (in case of a failure to find a suitable thermal during the gliding phase) is disproportionately higher for heavier birds in general (Pennycuick 2008) and in our 12 species as well, with mechanical power (W) at V_{mr} (the maximum range airspeed for flapping flyers) = 10.849 × body mass (kg) −1.556 ($R^2 = 0.980$, $P < 0.001$), and thus also greater for birds with higher wing loading. Altogether, birds with higher wing loading are more prone to the overall cost of the grounding/flapping risk. Indeed, variation in wing loading and its two components (body mass and wing area) may additionally reflect selective pressures for other fitness components other than long-distance migration such as reproductive success (Kullberg *et al*. 2002; Neto & Gosler 2010).

The grounding/flapping risk does not solely depend on bird morphology, but is also highly affected by environmental conditions. We found that soaring migrants changed their gliding airspeed in a risk-sensitive manner according to instantaneous conditions they encountered *en route*. Specifically, birds glided safer (i.e. closer to V_{bg}) when thermals were relatively weak (Fig. 4c) and when gliding started at lower elevation (Fig. 4d). Interestingly, the effect of altitude diminished above 1000 m height, suggesting that birds disregard risk due to gliding height above this threshold height, which may be perceived as an altitude allowing gliding birds to remain airborne for sufficient duration to safely locate a thermal during gliding. Whereas variation in wing loading is considered to reflect a major evolutionary response most notable at the interspecific level, variation in flight behaviour with regards to atmospheric conditions is considered to reflect a major ecological response of soaring organisms, most notable at the intraspecific level. Importantly, we show that both types of responses are modulated by risk-sensitive behaviour.

We show that two factors, wing loading and TKE, can be integrated in a quantitative way to predict variation in RAFI, representing key evolutionary and ecological factors affecting soaring-gliding flight (Fig. 5). Although other morphological traits and environmental conditions may affect risk-sensitive flight, we suggest that the strong effects of these two factors render them sufficient to construct a parsimonious model for the complex task of passive flight under substantial uncertainties and risks. We found that for our data set, variation in RAFI cannot be explained by tracking region (Idan or Sede Boqer, differing substantially in topography), year, season (spring vs. fall) or wind conditions (e.g. head-, tail- and cross-wind). Although other potentially influencing factors and data sets should be explored, we propose that this simple framework can be extrapolated beyond the species and sites included in our analysis.

Although the data set analysed in this study is substantially more comprehensive and variable than any bird soaring data set analysed in this context in terms of individuals, species, duration, and is also exceptional in terms of data quality and complementary atmospheric modelling, it still comes short-handed in answering some important aspects of soaring flight behaviour. For example, the lack of data on body mass and morphology at the individual level precludes direct tests of how intraspecific morphological differences affect risk-sensitive flight behaviour. Yet, we do show that our main results are robust to known variation in species' morphology (Fig. S3). In addition, the generality of the observed relationships should be re-examined over wider environmental variability incorporating also less or more extreme arid conditions than those experienced by our birds over the Negev Desert of Israel. Migrating birds crossing the Sahara, for instance, may be exceptionally risk averse due to the severe consequences of the grounding/flapping risk for bird survival (Klaassen *et al*. 2014). Furthermore, because radar data are inherently limited in their spatial extent, we could not explore variation in RAFI throughout continuous cross-country flight consisting of consecutive soaring-

gliding cycles. Analysis of longer tracks can help assess the scale at which birds can safely project the forthcoming thermal conditions from the conditions encountered in the current and previous soaring-gliding cycles. It can be predicted, for instance, that birds choose gliding airspeed not solely based on the climb rate (hence thermal intensity) they experienced in the last soaring phase, but integrate the climb rates experienced thus far, and perhaps respond to the trend, not just to the absolute values. Although we are not aware of an existing tracking system that can simultaneously record flight paths of multiple individuals within a relatively large area in a sufficiently high resolution, such data sets could elucidate if and how soaring-gliding performance of other birds nearby, conspecifics or from other species, affect the flight performance of individual birds. Moreover, tracking flight behaviour throughout the annual cycle will enable us to compare risk sensitivity in different ecological contexts, involving other movement types, such as central-place foraging during breeding (Spiegel *et al*. 2013) and long-range forays (Nathan *et al*. 2012).

In summary, our study illustrates the importance of combining high-resolution animal tracking data and atmospheric simulations for the study of the time and energy trade-offs that are essential for understanding the ecology and evolution of bird flight (Alerstam 1991; Hedenström 1993; Hedenström & Alerstam 1998; Alerstam *et al*. 2007; Pennycuick 2008; Bohrer *et al*. 2012) and of other major movement phenomena of airborne organisms (Isard & Gage 2001; Nathan *et al*. 2005). Furthermore, by corroborating both the growing attempts to understand intertwining evolutionary and ecological processes (Kokko & López-Sepulcre 2007; Schoener 2011) and the linkage between various internal and external components of the movement ecology of organisms (Nathan *et al*. 2008), our study shows how behaviour modulates the interface between ecology (response to environmental variation) and evolution (selection of morphological traits) in determining the flight performance of soaring-gliding migratory birds.

ACKNOWLEDGEMENTS

We thank the Swiss Ornithological Institute radar team, headed by B. Bruderer, and particularly M. Kestenholz, D. Peter, R. Spaar and H. Stark, who were responsible for the radar fieldwork. We would also like to thank T. Garland for advice on the phylogenetic analysis, and Adena Brickman, F. Bairlein, P. Berthold, I. Newton, C. Pennycuick, J. Shamoun-Baranes and three anonymous reviewers for their helpful remarks and suggestions. This project was supported by BSF grants 229/2002, 124/2004 and 255/2008, the Ring Foundation and the Robert Szold Fund, and the Minerva Center for Movement Ecology. The funders had no role in study design, data collection and analysis, decision to publish or preparation of the manuscript.

AUTHORSHIP

F. L. collected tracking data of the birds. N. H., I. M. and R. A. performed the atmospheric modelling. N. H., N. S. and R. N. conceived and designed the research, analysed the data and wrote the study.

REFERENCES

Ákos, Z., Nagy, M. & Vicsek, T. (2008). Comparing bird and human soaring strategies. *Proc. Natl Acad. Sci. USA*, 105, 4139–4143.

Ákos, Z., Nagy, M., Leven, S. & Vicsek, T. (2010). Thermal soaring flight of birds and unmanned aerial vehicles. *Bioinspir. Biomim.*, 5, 045003.

Alerstam, T. (1991). Bird flight and optimal migration. *Trends Ecol. Evol.*, 6, 210–215.

Alerstam, T. & Lindström, Å. (1990). *Bird Migration: Physiology and Ecophysiology*. Springer-Verlag, Berlin, Germany.

Alerstam, T., Rosén, M., Bäckman, J., Ericson, P.G.P. & Hellgren, O. (2007). Flight speeds among bird species: allometric and phylogenetic effects. *PLoS Biol.*, 5, e197.

Bohrer, G., Brandes, D., Mandel, J.T., Bildstein, K.L., Miller, T.A., Lanzone, M. *et al*. (2012). Estimating updraft velocity components over large spatial scales: contrasting migration strategies of golden eagles and turkey vultures. *Ecol. Lett.*, 15, 96–103.

Bradbury, T. (2000). Meteorology and Flight. A&C Black, London, UK.

Bruderer, B. & Boldt, A. (2001). Flight characteristics of birds: I. radar measurements of speeds. *Ibis*, 143, 178–204.

Bruderer, B., Underhill, L.G. & Liechti, F. (1995). Altitude choice by night migrants in a desert area predicted by meteorological factors. *Ibis*, 137, 44–55.

Bruderer, B., Peter, D., Boldt, A. & Liechti, F. (2010). Wing-beat characteristics of birds recorded with tracking radar and cine camera. *Ibis*, 152, 272–291.

Burnham, K.P. & Anderson, D.R. (2002). *Model Selection and Multi-Model Inference: A Practical Information-Theoretic Approach*. Springer, New York, NY, USA.

Cotton, W.R., Pielke, R.A., Walko, R.L., Liston, G.E., Tremback, C.J., Jiang, H. *et al*. (2003). RAMS 2001: current status and future directions. *Meteorol. Atmos. Phys.*, 82, 5–29.

Del Hoyo, J., Elliott, A., Sargatal, J. & Cabot, J. (1992). *Handbook of the Birds of the World*. Lynx Edicions, Barcelona, Spain.

Duerr, A.E., Miller, T.A., Lanzone, M., Brandes, D., Cooper, J., O'Malley, K. *et al*. (2012). Testing an emerging paradigm in migration ecology shows surprising differences in efficiency between flight modes. *PLoS ONE*, 7, e35548.

Ellington, C.P. (1984). The aerodynamics of hovering insect flight. IV. aeorodynamic mechanisms. *Philos. Trans. R. Soc. Lond. B*, 305, 79–113.

Garland, T. & Ives, A.R. (2000). Using the past to predict the present: confidence intervals for regression equations in phylogenetic comparative methods. *Am. Nat.*, 155, 346–364.

Griffiths, C.S., Barrowclough, G.F., Groth, J.G. & Mertz, L.A. (2007). Phylogeny, diversity, and classification of the Accipitridae based on DNA sequences of the RAG-1 exon. *J. Avian Biol.*, 38, 587–602.

Hackett, S.J., Kimball, R.T., Reddy, S., Bowie, R.C.K., Braun, E.L., Braun, M.J. *et al*. (2008). A phylogenomic study of birds reveals their evolutionary history. *Science*, 320, 1763–1768.

Hedenström, A. (1993). Migration by soaring or flapping flight in birds: the relative importance of energy cost and speed. *Philos. Trans. R. Soc. Lond. B*, 342, 353–361.

Hedenström, A. & Alerstam, T. (1998). How fast can birds migrate? *J. Avian Biol.*, 29, 424–432.

Hedenström, A., Johansson, L.C., Wolf, M., Von Busse, R., Winter, Y. & Spedding, G.R. (2007). Bat flight generates complex aerodynamic tracks. *Science*, 316, 894–897.

Isard, S.A. & Gage, S.H. (2001). *Flow of Life in the Atmosphere: An Airscape Approach to Understanding Invasive Organisms*. Michigan State Univ Press, East Lansing, MI, USA.

Kerlinger, P. (1989). *Flight Strategies of Migrating Hawks*. University of Chicago Press, Chicago, IL, USA.

Klaassen, R.H.G., Hake, M., Strandberg, R., Koks, B.J., Trierweiler, C., Exo, K.M. *et al*. (2014). When and where does mortality occur in migratory birds? Direct evidence from long-term satellite tracking of raptors. *J. Anim. Ecol.*, 83, 176–184.

Kokko, H. & López-Sepulcre, A. (2007). The ecogenetic link between demography and evolution: can we bridge the gap between theory and data? *Ecol. Lett.*, 10, 773–782.

Kullberg, C., Metcalfe, N.B. & Houston, D.C. (2002). Impaired flight ability during incubation in the pied flycatcher. *J. Avian Biol.*, 33, 179–183.

Liechti, F. (2006). Birds: blowin'by the wind? *J. Ornithol.*, 147, 202–211.

Liechti, F., Ehrich, D. & Bruderer, B. (1996). Flight behaviour of white storks *Ciconia ciconia* on their migration over southern Israel. *Ardea*, 84, 3–13.

MacCready, P. B. (1958). Optimum airspeed selector. *Soaring*, Jan-Feb, 10–11.

Mandel, J.T., Bildstein, K.L., Bohrer, G. & Winkler, D.W. (2008). Movement ecology of migration in turkey vultures. *Proc. Natl Acad. Sci. USA*, 105, 19102–19107.

Nathan, R., Sapir, N., Trakhtenbrot, A., Katul, G.G., Bohrer, G., Otte, M. *et al.* (2005). Long-distance biological transport processes through the air: can nature's complexity be unfolded *in silico? Divers. Distrib.*, 11, 131–137.

Nathan, R., Getz, W.M., Revilla, E., Holyoak, M., Kadmon, R., Saltz, D. *et al.* (2008). A movement ecology paradigm for unifying organismal movement research. *Proc. Natl Acad. Sci. USA*, 105, 19052–19059.

Nathan, R., Spiegel, O., Fortmann-Roe, S., Harel, R., Wikelski, M. & Getz, W.M. (2012). Using tri-axial acceleration data to identify behavioral modes of free-ranging animals: general concepts and tools illustrated for griffon vultures. *J. Exp. Biol.*, 215, 986–996.

Neto, J.M. & Gosler, A.G. (2010). Variation in body condition of breeding Savi's Warblers *Locustella luscinioides*: the reproductive stress and flight adaptation hypothesis revisited. *J. Ornithol.*, 151, 201–210.

Nilsson, C., Klaassen, R.H.G. & Alerstam, T. (2013). Differences in speed and duration of bird migration between spring and autumn. *Am. Nat.*, 181, 837–845.

Pennycuick, C.J. (1969). The mechanics of bird migration. *Ibis*, 111, 525–556.

Pennycuick, C.J. (1972). Soaring behaviour and performance of some East African birds, observed from a motor-glider. *Ibis*, 114, 178–218.

Pennycuick, C.J. (1978). Fifteen testable predictions about bird flight. *Oikos*, 30, 165–176.

Pennycuick, C. J. (2008). *Modelling the Flying Bird*. Elsevier, Amsterdam [etc.].

Pielke, R.A., Cotton, W.R., Walko, R.L., Tremback, C.J., Lyons, W.A., Grasso, L.D. *et al.* (1992). A comprehensive meteorological modeling system—RAMS. *Meteorol. Atmos. Phys.*, 49, 69–91.

Reichmann, H. (1978). *Cross-Country Soaring*. Thomson, Santa Monica, CA, USA.

Sapir, N., Horvitz, N., Wikelski, M., Avissar, R., Mahrer, Y. & Nathan, R. (2011). Migration by soaring or flapping: numerical atmospheric simulations reveal that turbulence kinetic energy dictates bee-eater flight mode. *Philos. Trans. R. Soc. Lond. B*, 278, 3380–3386.

Schoener, T.W. (2011). The newest synthesis: understanding the interplay of evolutionary and ecological dynamics. *Science*, 331, 426–429.

Spaar, R. & Bruderer, B. (1996). Soaring migration of Steppe Eagles *Aquila nipalensis* in southern Israel: flight behaviour under various wind and thermal conditions. *J. Avian Biol.*, 27, 289–301.

Spaar, R. & Bruderer, B. (1997). Migration by flapping or soaring: flight strategies of Marsh, Montagu's and Pallid Harriers in southern Israel. *Condor*, 99, 458–469.

Spiegel, O., Harel, R., Getz, W.M. & Nathan, R. (2013). Mixed strategies of griffon vultures'(*Gyps fulvus*) response to food deprivation lead to a hump-shaped movement pattern. *Movement Ecol.*, 1, 5.

Stull, R.B. (1988). *An Introduction to Boundary Layer Meteorology*. Springer, New York, NY, USA.

Tucker, V.A. (1987). Gliding birds: the effect of variable wing span. *J. Exp. Biol.*, 133, 33–58.

Vogel, S. (1966). Flight in *Drosophila* I. Flight performance of tethered flies. *J. Exp. Biol.*, 44, 567–578.

Walko, R.L., Band, L.E., Baron, J., Kittel, T.G.F., Lammers, R., Lee, T.J. *et al.* (2000). Coupled atmosphere-biophysics-hydrology models for environmental modeling. *J. Appl. Meteorol.*, 39, 931–944.

SUPPORTING INFORMATION

Additional Supporting Information may be downloaded via the online version of this article at Wiley Online Library (www.ecologyletters.com).

Editor, Marcel Holyoak
Manuscript received 2 October 2013
First decision made 2 November 2013
Second decision made 11 February 2014
Manuscript accepted 17 February 2014